Langmuir

Article

pubs.acs.org/Langmuir

Action at a Distance: Functional Drug Delivery Using Electromagnetic-Field-Responsive Polypyrrole Nanowires

Wen Gao,[†] Jianming Li,[†] John Cirillo,[†] Richard Borgens,*[,†,‡] and Youngnam Cho*[,†,§]

[†]Center for Paralysis Research, Department of Basic Medical Sciences, College of Veterinary Medicine and [‡]Weldon School of Biomedical Engineering, College of Engineering, Purdue University, West Lafayette, Indiana 47907, United States

[§]New Experimental Therapeutic Branch, National Cancer Center, 111 Jungbalsan-ro, Ilsandong-gu, Goyang, Gyeonggi-do 410-769, South Korea

Supporting Information

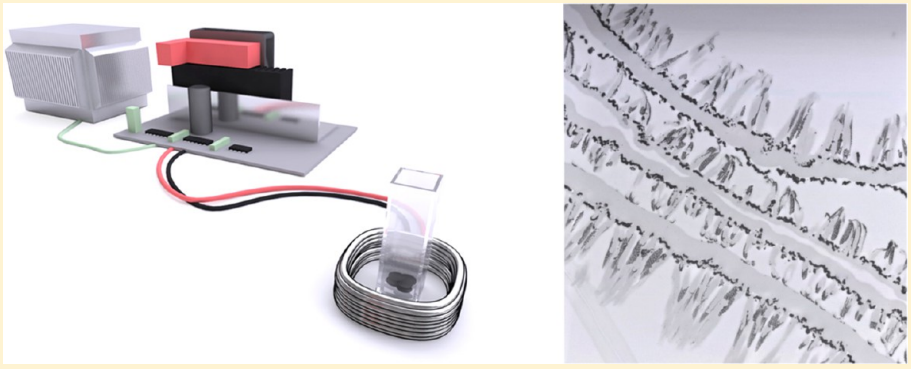

ABSTRACT: In this work, we introduce a free-standing, vertically aligned conductive polypyrrole (Ppy) architecture that can serve as a high-capacity drug reservoir. This novel geometric organization of Ppy provides a new platform for improving the drug-loading efficiency. Most importantly, we present the first formal evidence that an impregnated drug (dexamethasone, DEX) can be released on demand by a focal, pulsatile electromagnetic field (EMF). This remotely controlled, on−off switchable polymer system provides a framework for implantable constructs that can be placed in critical areas of the body without any physical contact (such as percutaneous electrodes) with the Ppy, contributing to a low "foreign body" footprint. We demonstrate this possibility by using a BV-2 microglia culture model in which reactive oxygen species (ROS) and inducible nitric oxide synthase (iNOS) expression was attenuated in response to DEX released from EMF-stimulated Ppy.

1. INTRODUCTION

There are growing clinical demands for controlled and sustained drug release systems to serve as implantable devices for patients with acute and chronic diseases. Under these circumstances, it is not surprising that intelligent materials have emerged as a promising strategy for drug delivery. For example, many efforts have been directed toward using various stimuli-responsive biomaterials as "on−off" controllable drug carriers in which the bioactive cargos are released via changes in pH, temperature, or input of electrical or UV energy.[1−3] At the present time, electrical stimulation appears to be one of the more suitable approaches for clinical translation in that (1) the electrical signal can be triggered using portable equipment, not requiring significant cost or sophisticated technologies, and (2) the generated signal can be tuned using a variety of exposure times and current intensities. In this regard, conductive polymers have emerged as one of the more useful drug-delivery platforms.

In particular, polypyrrole (Ppy) has become a candidate material due to its lack of toxicity, favorable biocompatibility, and reversible electrochemical properties.[4,5] For instance, polypyrrole demonstrated excellent in vivo biocompatibility, with results similar to Teflon when implanted as a neural prosthetic.[4] Both glial and neuronal cells were found to be in intimate contact with the Ppy material. Other studies noted that PPy extracts exhibited no hemolytic, allergenic, or mutagenic properties whereas sciatic nerve implants elicited only a minor inflammatory response 6 months postimplantation.[6]

Functionally, the electrostatic interaction of Ppy in response to electric current provides a controllable "switch" for the release of tethered cargo, providing in situ delivery of nerve growth factors, anti-inflammatory drugs, or adenosine triphosphate.[7−10] Prior investigations demonstrate that time- and site-specific release profiles can be obtained by modifying electrical or magnetic pulse patterns and durations.[11−13] Electromagnetic fields (EMF) have been further discussed as another potential form of stimulus for drug delivery and was first realized in carbon nanotubes.[14]

We have previously outlined the fabrication and physiochemical details that advance the potential of Ppy in medical practice.[15]

Received: January 13, 2014
Revised: May 21, 2014
Published: June 9, 2014

   dx.doi.org/10.1021/la500033b | *Langmuir* 2014, 30, 7778−7788

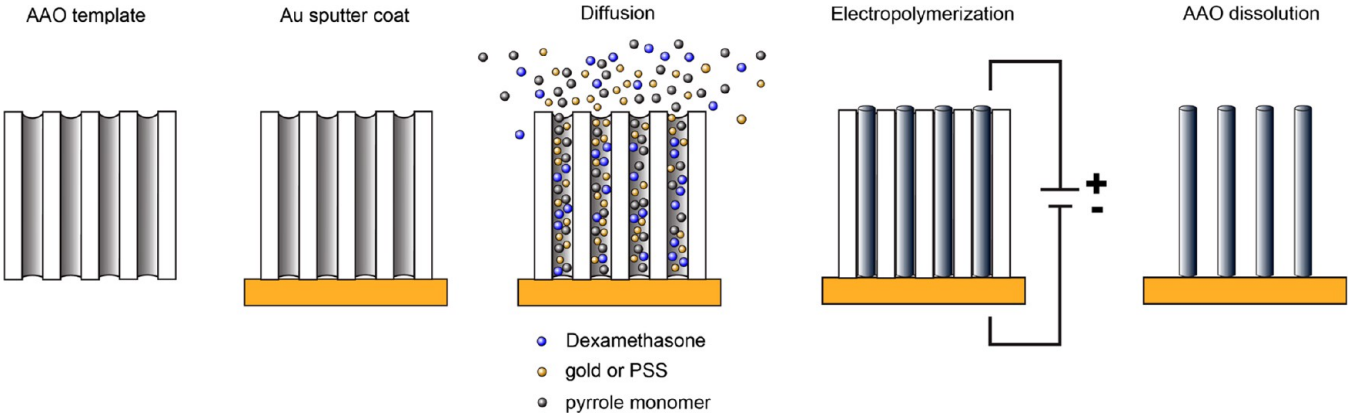

Figure 1. Overview of nanowire fabrication. Stepwise preparation is from left to right. Each cutaway diagram is an illustration of the AAO template. At the far left, the illustration of the AAO template is shown. Next, the template is coated with gold on one side. The third step illustrates the filling and diffusion of the solution consisting of pyrrole monomer, AuNps or PSS, and DEX in the template pores. The fourth step is the DEX-conjugated polypyrrole electropolymerization process. Finally (far right), the Ppy NWs are shown attached to the gold base after the dissolution of the AAO template with sodium hydroxide.

However, two obstacles that prevent the practical use of the Ppy polymer systems are the following: (1) the amount of a drug's cargo is limited when using typical flat thin-film fabrication and (2) delivery of the cargo within the human body requires percutaneous electrodes to deliver the required level of electric current (i.e., a physical electrical contact with the Ppy substrate). This latter obstacle must be understood in the context of chronic applications where drug release may be desirable over many days until the supply within the film is exhausted. During this time, percutaneous wires carry the possibility of infection by retrograde tracking along the insertion path where normal movement vitiates a perfect seal between tissues and the insulated electrodes.[16]

In this work, we detail a new Ppy paradigm that overcomes the limits of payload and invasive delivery. We demonstrate that a three-dimensionally nanostructured Ppy platform impregnated with a model test drug (dexamethasone, DEX)[17,18] exhibits outstanding drug loading efficiency. Moreover, noninvasive and on-demand drug release has been demonstrated by exposing the Ppy nanowires to high-frequency pulsed electromagnetic fields (EMF). Subsequent studies using a lipopolysaccharide-challenged BV-2 glial cell line showed that the DEX released by EMF stimulation remained bioactive and ameliorated both oxidative damage and the inflammatory response. The putative inductive coupling between the DEX-doped polypyrrole nanowires (DEX/PpyNWs) and EMFs bypasses the requirement for direct electrical contact with Ppy and opens the door to Ppy embodiments that can be placed in vivo in which the cargo can be delivered controllably and noninvasively for many weeks.

2. MATERIALS AND METHODS

2.1. Template Preparation. Ppy flat films and nanowires were fabricated using common electropolymerization techniques. The first step in this manufacturing process was the preparation of the templates. For flat PPy films, indium tin oxide (ITO) glass slides with 5−15 Ω resistivity (Delta Technologies) were washed in acetone for 30 min, followed by ethanol and Milli-Q water in an ultrasonic bath. For PpyNWs experiments, an anodic aluminum oxide template (AAO, Figure 1) with a 0.2 μm pore size and 60 μm thickness (Whatman) was obtained. The AAO templates were subsequently coated with a 100-nm-thick gold layer on one side using a Varian E-beam evaporator. All templates were stored in a dry oven prior to use.

2.2. Fabrication of Ppy-DEX Carriers. Following template making, the electrolytic solutions were prepared. Briefly, an aqueous mixture consisting of 0.2 M pyrrole (Py, Sigma), 0.025 M dexamethasone 21-phosphate disodium salt (DEX, Sigma), and 0.05 M 10 nm NanoXact spherical gold nanoparticles (AuNps, NanoComposix, CA) was mixed. For comparison, 0.2 M pyrrole, 0.025 M DEX, and 0.1 M poly(3,4-ethylenedioxythiophene)-poly(styrenesulfonate) (PSS, Sigma) were also mixed for synthesis. Note that for the in vitro experiment the concentration of DEX within the solutions was decreased to 5 mM. Prepared AAO templates were subsequently incubated into their respective mixtures for 30 min. Cleaned ITO slides and AAO templates were separately connected to the working electrode from a CH Instruments model 604 electrochemical analyzer/workstation, with a platinum counter electrode and Ag/AgCl reference electrode placed in the synthesis solution. The one-step electropolymerization of DEX/Ppy was accomplished by applying a constant potential of 1 V using a potentiostat. Following polymerization, the final films were rinsed thoroughly with Milli-Q water for 5 min. The AAO templates were removed by placing the films in 3 M sodium hydroxide and then rinsed with Milli-Q water.

2.3. Scanning and Transmission Electron Microscopy. Ppy samples were prepared by first sputter coating with platinum for 60 s. SEM images were taken with an FEI NOVA nano SEM via field emission scanning using ET and TLD at high vacuum at an acceleration voltage of 5 kV. TEM images were taken using a FEI/Philips CM-10 transmission electron microscope operated at 100 kV, a 200 μm condenser aperture, and a 70 μm objective aperture. TEM images were captured with an SIA L3-C digital camera.

2.4. Electromagnetic Stimulation of Ppy. Multiple factors must be considered when designing the EMF stimulation system and pulse conditions. These parameters include the waveform shape, pulse duration, pulse magnitude, duty cycle, and so forth. We originally chose a narrow pulse width (500 nS) stimulating regime as it allowed us to experiment with various coil geometries with minimal power consumption. The square wave was chosen in order to maximize the induced electric fields within the Ppy since that is the hypothesized stimulus for drug release. Our original pilot measurements were made using a three-turn coil which had a very low inductance allowing testing that set the limits for overheating. This data (not shown) then permitted the construction of a 15-turn coil, which was used in all experiments reported here. Briefly, AWG 16 copper wire was wound 15 times to create a 15-turn coil. The geometry of the coil was 2.3 × 2.8 cm^2 inside dimensions and 3.0 × 3.8 cm^2 outside dimensions. The height of the coil was 1.2 cm (Figure 2). The coil was then stimulated with a pulsing regime using a custom-made circuit. Each input pulse was on only long enough to saturate the coil and then was turned off for the duration required to unload the coil completely (~10 μS). Therefore, the duty cycle was approximately 4.8%. Additionally, we tested several stimulation patterns such as oscillating the polarity, grouping the same polarity

dx.doi.org/10.1021/la500033b | Langmuir 2014, 30, 7778−7788

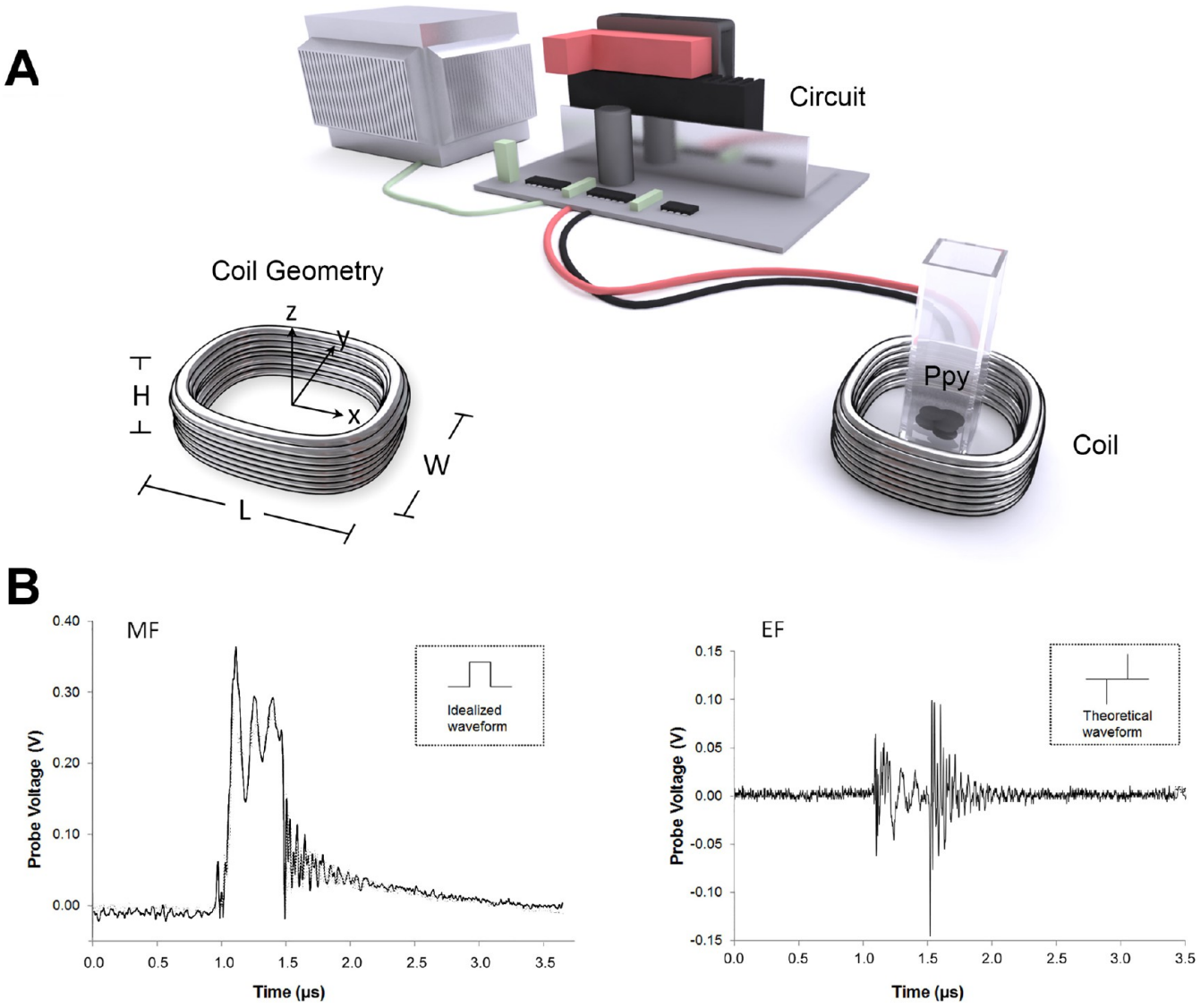

Figure 2. Stimulation scheme for the application of EMFs. (A) The top illustration shows the integrated system used to create the electromagnetic field (EMF) to induce PpyNWs activity. The stimulator is connected to a wire-wound coil in which a standard cuvette is placed in the center. Polypyrrole samples were loaded in the cuvette and submerged in a buffer solution. Following EMF stimulation, aliquots of the solution were assayed for drug concentration via UV−vis spectrophotometry. The left inset describes the dimensions of the stimulating coil, where H = 1.2 cm, L = 3.8 cm, and W = 3.0 cm. The recordings in (B), left and right, are probe measurements of the magnetic fields (MF) and electric fields (EF) at the center of the coil (∼36 G and 4000 V/m, respectively). The insets describe the idealized MF and EF waveforms based on the input square-pulse stimulation regime.

pulses in different temporal patterns, and so forth while maintaining a ∼5% duty cycle. As we did not find significant differences in drug release in the initial trials (data not shown), we utilized the waveform described in Figure S2 in order to minimize heat generation.

2.5. EMF Measurements. Using the waveform patterns in Figure S1 as the input signal, the real time magnetic and electric field outputs from the stimulation coil were measured using high-frequency EMC 100B (magnetic) and 100D (electric) probes (Beehive Electronics, CA). Probes were connected to a Tektronics TDS 2012B oscilloscope and terminated with a 50 Ω resistor. For data collection, each probe was positioned in the stimulation coil center (origin). The probes were directional and oriented in the direction of the maximum expected reading. This value was taken to be the output probe value and was converted to dBm. The recorded data points from the oscilloscope were imported into MS Excel in which the fast Fourier transform (FFT) of the waveforms was calculated. From the FFTs, the fundamental frequency and with the output dBm power value were used with the antenna gain equation (Figure S1) provided for each probe to estimate ac field magnitudes.

2.6. DEX Release. Both potentiostat electrical stimulation and pulsed EMF applications were used to release DEX. In former cases, the setup was the same as for the electropolymerization process with three electrodes, but the DEX-conjugated Ppy film was connected to a working electrode and subsequently placed in PBS solution containing 0.80% w/v NaCl. A constant voltage of −0.1 V was applied for 5 h using a CH Instruments model 604 electrochemical analyzer/workstation. For comparison, the DEX/Ppy platforms were also stimulated by an induced EMF generated by our custom circuit and coil stimulator system. The supernatants were collected after 1, 3, and 5 h of stimulation for both the potentiostat and the pulsed magnetic field generator. Figure 2 depicts the experimental setup and the essential components of the EMF stimulation system used to remotely trigger Ppy drug release. The Ppy samples were placed in a 12.5 mm × 12.5 mm × 45 mm standard cuvette filled with phosphate buffer solution. The cuvette was positioned in the center void of the stimulation coil but was not in physical contact with the coil. The coil was subsequently energized using square wave pulse trains as described in Figure S1.

dx.doi.org/10.1021/la500033b | *Langmuir* 2014, 30, 7778−7788

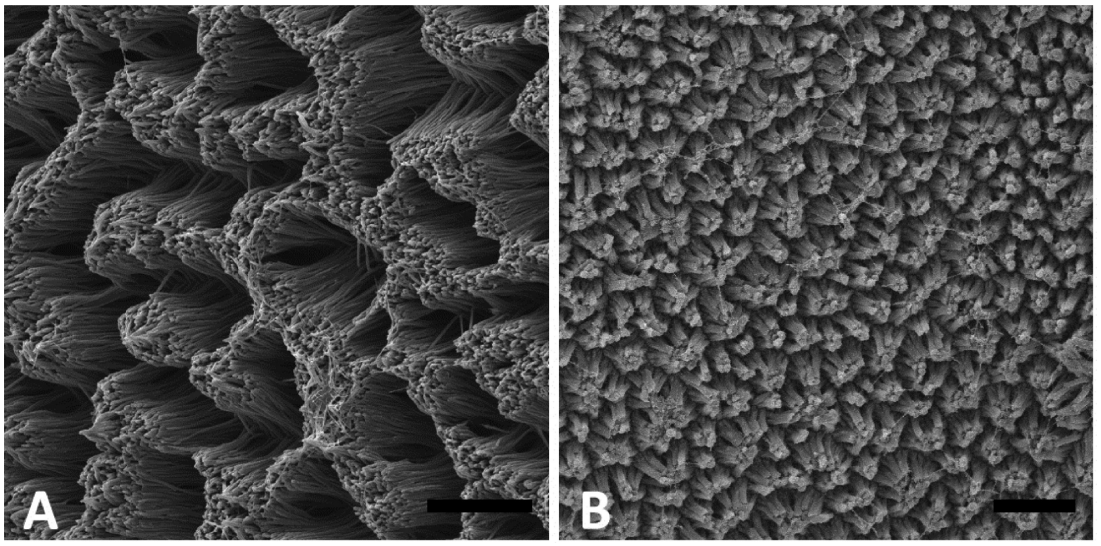

Figure 3. (A) Scanning electron micrograph showing a top (dorsal) view of polypyrrole wires (200 nm diameter and 10 μm length) produced with 1300−1400 s of deposition. (B) A similar micrograph where 200−300 s of deposition was used. Scale bars: (A) 10 μm and (B) 2 μm.

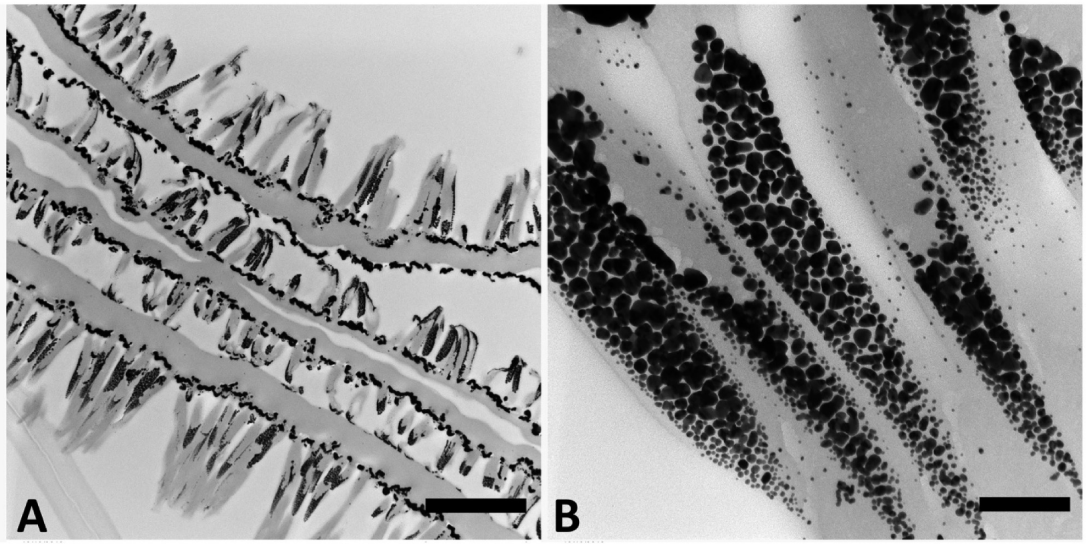

Figure 4. (A) Transmission electron micrograph of individual nanowires projecting from gold bases. Note that several gold bases are shown due to the folding of the PpyNWs. The dark regions near the base to midsection are gold nanoparticle deposits. (B) Higher-magnification TEM of individual nanowires showing the details of gold nanoparticle deposition. These wires range from approximately 500 to 2000 nm in length and 150 nm in diameter. Scale bars: (A) 2 μm and (B) 0.2 μm.

Experiments comparing the DEX-conjugated polypyrrole compositions and the drug release effects of stimulation were continued for up to 16 days using EMF stimulation. To test if the stimulated release of DEX might be influenced by the heating of stimulated samples, we placed the DEX-doped flat polypyrrole templates within a controlled incubator at 37 °C. This temperature was slightly higher than ambient temperature in the vicinity of the active coil, which was measured to be about 30 °C. For all 16 days of DEX release, the sample solutions were collected after 1, 3, 5, 7, 10, 13, and 16 days of continuous EMF stimulation (n = 5). All collected aliquot samples were analyzed with a UV−vis spectrometer at a 242 nm wavelength. A calibration curve of DEX (y(OD) = 23.8x − 0.04) was also prepared to detect the drug release.

2.7. Testing on Demand DEX Release from PpyNWs. To determine the characteristics of pulsatile EMF stimulation, "on and off" experiments were performed on polypyrrole nanowires synthesized with gold nanoparticle (PpyNWs−AuNps) samples. The DEX release profile recordings were begun after 10 h of stimulation by the pulsed EMF. Then, pulsed EMF stimulation was turned on (referred to as the on time) for 2 h and discontinued (off time) for 2 h. This regimen was continued for four cycles for each sample.

2.8. XPS Analysis. Ppy samples of about 0.5−1.0 cm^2 were prepared and submitted for XPS analysis. The surface chemical composition of the samples was analyzed by X-ray photoelectron spectroscopy (XPS) using a Kratos Axix Ultra DLD spectrometer. The spectra were collected using monochromatic Al Kα radiation (1486.6 eV). The survey and high-resolution spectra were obtained in constant pass energy mode with pass energies of 160 and 20 eV, respectively (survey, 1 eV/step; high-resolution spectra, 0.05 eV/step). A built-in Kratos charge neutralizer was used. Data analysis was performed with CasaXPS software version 2.3.12.

2.9. ROS Detection in Challenged BV-2 Cells. The BV-2 cells were cultured in 75 cm^2 flasks in Dulbecco's modified Eagle's medium (Sigma-Aldrich) with 10% fetal bovine serum, 100 IU/mL penicillin, and 100 μg/mL streptomycin. Cells were maintained at 37 °C in a humidified incubator with 5% CO_2, harvested by trypsinizing (0.25% trysin/EDTA in PBS), and reseeded (at approximately 1 × 10^6 density) in 12-well dishes for 24 h to detect ROS. Cells were incubated in the

dx.doi.org/10.1021/la500033b | Langmuir 2014, 30, 7778−7788

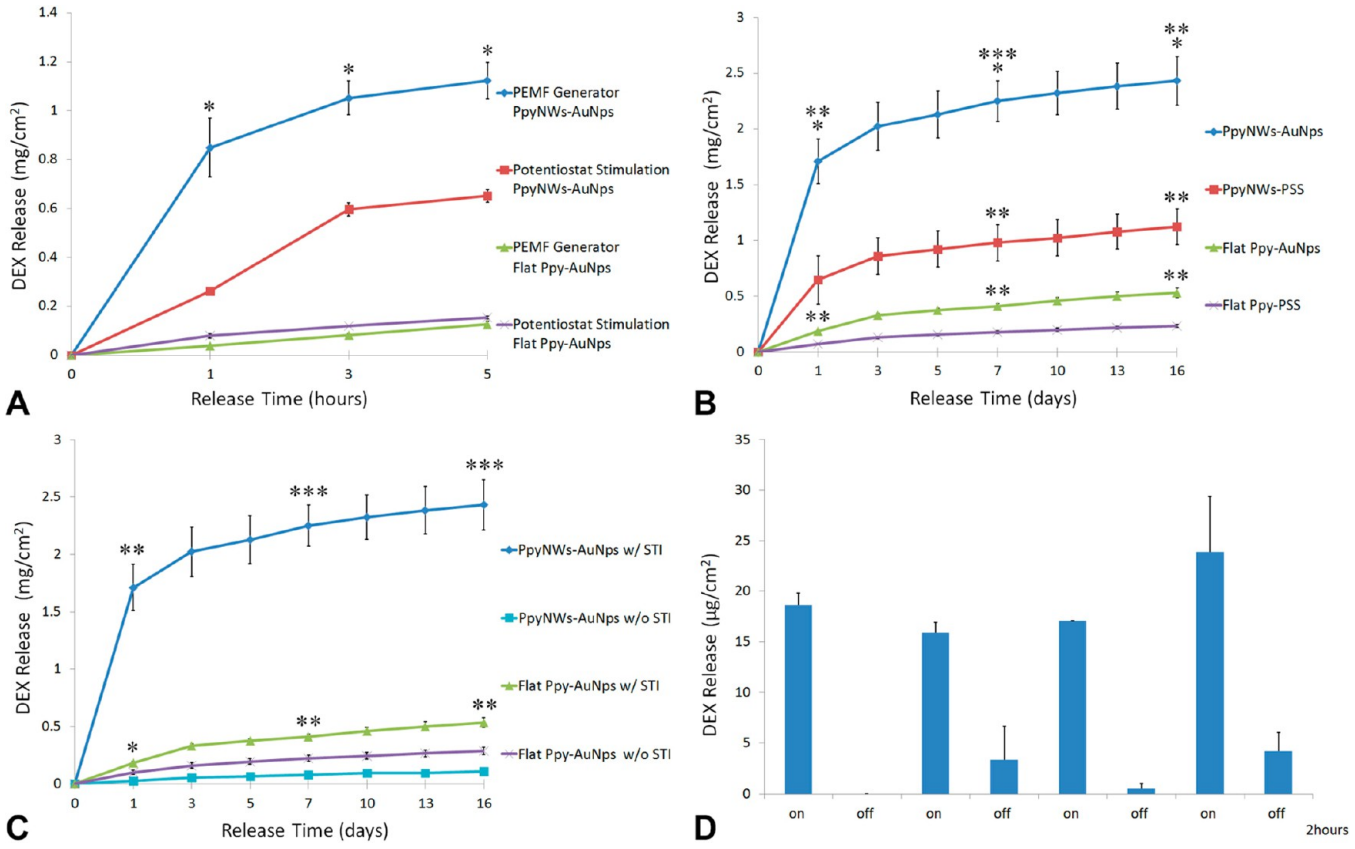

Figure 5. UV−Vis spectrophotometric comparison of DEX release from various Ppy platforms. (A) The release profiles of DEX from both a conventional flat Ppy film and Ppy NWs within 5 h, with one group stimulated electrically using a potentiostat and the others by EMF. (B) Comparison between gold nanoparticles vs PSS dopants using EMF stimulation. Again, there was only marginal release of DEX (<0.5 mg/cm^2) from flat Ppy films. (C) Active (EMF stimulation) vs passive (no stimulation) of both flat Ppy films and PpyNWs. Note that an extraordinary release of DEX occurs after EMF stimulation of the PpyNW-AuNps. (D) Bar graph demonstrating the switchable nature of PpyNWs-AuNps. High concentrations of DEX were produced by EMF stimulation. The small amount of DEX detected at the off times was likely due to passive diffusion from the source. An approximately 8-fold increase in DEX release was achieved by EMF. *$P \leq 0.05$, **$P \leq 0.01$, and ***$P \leq 0.001$.

medium containing 1μg/mL lipopolysaccharides (LPS) from *Escherichia coli* 026:B6 (Sigma-Aldrich) for 6 h.[19] Then, BV-2 cells were treated with 1 μg/mL DEX after the application of LPS for 1 h. To detect DEX release by pulsed EMF, PpyNWs-AuNps films (approximately 30-40 mm^2 in unit area) were stimulated for 30 min and 1 h after LPS treatment in 1 h increments. In these experiments, the coil was placed flat directly below the Petri dish, aligned with the well and touching the bottom surface of the dish. Control wells did not receive EMF stimulation. After 6 h of LPS treatment, cells were trypsinized, centrifuged, and resuspended in a 10 μM oxidative stress indicator (CM-H2DCFDA, Molecular Probes) in PBS. Suspended cells were then placed in the incubator for 1 h, and the measurement of ROS was performed with a plate reader at 480 nm/530 nm. Measurement was also performed with a fluorescence microscope (Olympus IX 81 inverted). The cells were illuminated with an X-Cite series 120PCQ fluorescence illumination source. Additionally, another strong oxidizing reagent, hydrogen peroxide (H_2O_2), was used to confirm the LPS results (OxiSelect Intracellular ROS assay kit; Cell Biolabs, Inc.). Briefly, BV-2 cells were seeded in black 96-well plates for 12 h and then incubated in 1 mM DCFH-DA solution for 1 h. Hydrogen peroxide (20 μM) was incubated in these plates for 30 min, and then DEX treatments were applied for 15 min. For EMF-stimulated DEX release, the PpyNWs-AuNps films were divided into smaller pieces (approximately 30 mm^2), placed in each well, and stimulated for 15 min. In these instances, the coil was placed below the 96-well plate touching the bottom surface, with wells in a 3 × 3 matrix being stimulated. The fluorescence of all samples was read using a fluorescence plate reader.

2.10. Immunofluorescence Labeling Assay. BV-2 cells were cultured on poly-D-lysine (Sigma) precoated round cover glasses (no. 1.5 thickness, 12 mm) in 12-well plates for 24 h. After experimental treatment with LPS, DEX, and released DEX, BV-2 cells were fixed with 4% paraformaldehyde for 30 min at room temperature. A blocking solution, 1% albumin from bovine serum (Sigma-Aldrich), was applied to the samples for 1 h. Antinitric oxide synthase II antibody (EMD Millipore) was diluted in a ratio of 1:400 with antibody dilution buffer (Sigma). Cells were then incubated in a diluted primary antibody solution overnight at 4 °C. The next day, these cells were incubated in 1:100 diluted Cy3 conjugated goat antirabbit IgG antibody solution (EMD Millipore) for 2 h. Dried cover glasses were mounted on glass slides using a vectashield hardset mounting medium with DAPI (Vector Lab). These samples were all imaged with a confocal microscope (Leica SP5/STED/MP system).

2.11. Statistical Analysis. All of the data are shown with the standard error of the mean ± SEM. Comparative tests used were the conventional student's *t* test and one-way ANOVA, with significance determined by a *P* value of ≤0.05.

3. RESULTS

3.1. Structure of Polypyrrole Nanowires. Nanowire architecture was revealed by SEM and TEM (Figures 3 and 4). The length of grown PpyNWs is dependent on the polymerization time. Polypyrrole wires (10 μm long) were completed in about 1300−1400 s of deposition using the potentiostat (Figure 2A), while shorter lengths were realized for shorter deposition times (Figure S3B). The desired structure of PpyNWs was achieved for 200−300 s of deposition (Figure 3B). As an aside, smaller PpyNWs can also be fabricated. PpyNWs (200 nm long) were

dx.doi.org/10.1021/la500033b | *Langmuir* 2014, 30, 7778−7788

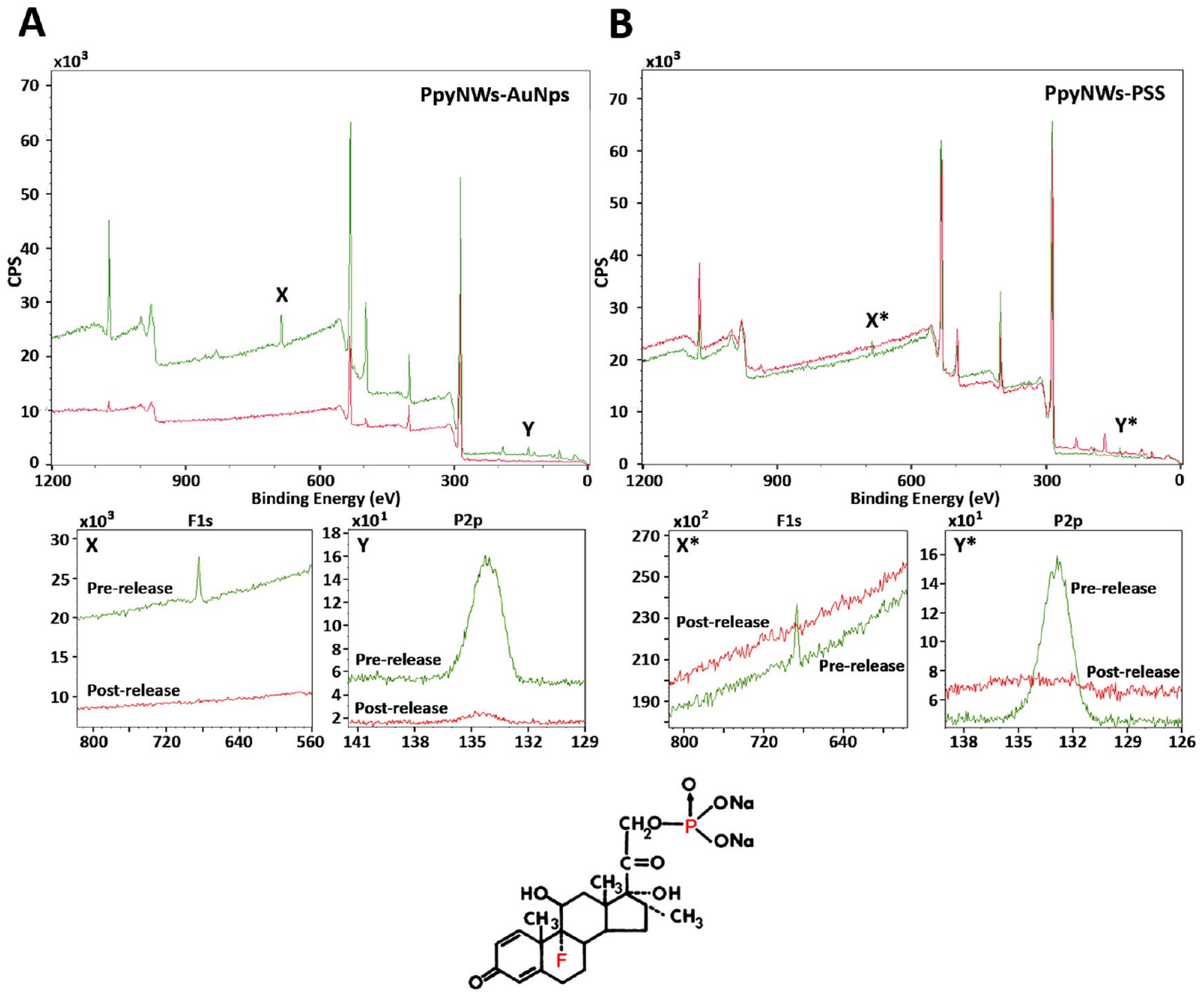

Figure 6. XPS spectra for the surface analysis of the DEX presence on Ppy templates before and after pulsed EMF stimulation. (A) XPS recording of DEX-doped PpyNWs-AuNps before (green) and after (red) DEX release by EMF. Characteristic peaks are shown in this spectrograph. (B) XPS data of DEX-doped PpyNWs-PSS before (green) and after (red) 16 days of EMF stimulation. Below, A and B are expanded views of these same records. These show details of signature fluorine and phosphorus elements in the DEX molecule before stimulation, respectively. Note that these elemental signatures vanish after EMF stimulation, indicative of DEX release from the surface. The bottom graph shows the molecular structure of DEX, with fluorine (F) and phosphorus (P) highlighted in red.

fabricated using different AAO templates with 0.02 μm pores (Figure S3A), but these were not used in this study. The free-standing, vertically aligned PpyNWs were generally arranged into mats in unit areas of up to 1 to 2 cm^2.

Figure 4A,B shows the distribution of gold nanoparticles within the bulk of 500-nm- to 2-μm-long PpyNWs.

3.2. EMF Characteristics. The real-time magnetic and electric field output waveforms at the coil center were plotted in Figure 2. The measurements revealed that the magnetic field output was similar to the input field, with some oscillation noise present in the square waveform. FFT decomposition of the measured signal showed that the fundamental frequency of the magnetic field was 3.2 MHz. This converts to an average peak amplitude of 36 G when using the antenna gain equation supplied by the probe vendor (Figure S1). Moreover, the amplitude of the magnetic field did not vary by more than 20% within the coil. The highest field amplitudes were located near the corners in the $x-y$ plane containing the coil center. Along the z axis, there was a small decrease in intensity as the probe was moved away from the coil center. Overall, the magnetic field was focused and concentrated within the internal space of the coil. However, outside of the coil, the magnetic field became divergent and weak, with the field roughly following a cubic decay. Therefore, Ppy drug-release experiments were tested with the films situated within the coil. On the basis of the obtained MF probe readings, the Ppy films were exposed to peak magnetic fields within the range of 25−40 G.

Similarly, the raw electric field data obtained for each coil is also depicted in Figure 2B. Note that the measured electric field corresponded to the derivative of the measured magnetic field, as expected by Faraday's law. The electric field waveform exhibited oscillatory behavior with sharp peaks primarily concentrated in the "ramp-up" and "switch off" phases of the EMF. The 15-turn coil produced a peak E field of 4700 V/m and a fundamental frequency of 65 MHz. Thus, the estimated electric field magnitude in which the Ppy fabrications resided is in the

dx.doi.org/10.1021/la500033b | Langmuir 2014, 30, 7778−7788

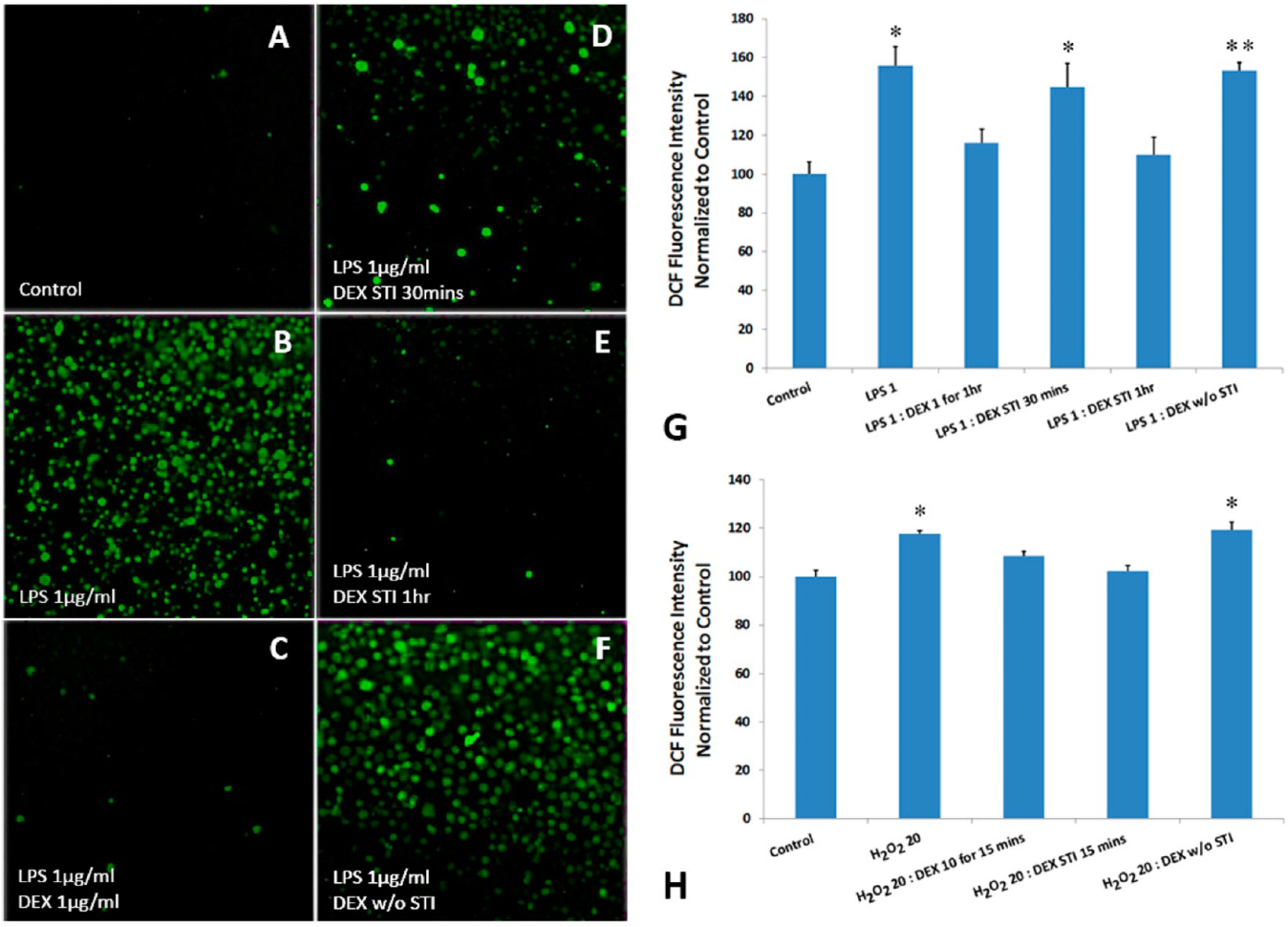

Figure 7. Composite fluorescence images and quantitative measurement of ROS. (A) Control without LPS insult. (B) BV-2 cells insulted by LPS, with intense green labeling of ROS by 2′,7′-dichlorodihydrofluorescein (DCF). (C) ROS was eliminated by the direct introduction of 1 μg/mL DEX suspended in the medium. (D) 30 min of EMF stimulation from DEX-doped PpyNWs-AuNps, demonstrating reduced ROS production. (E) With 1 h of EMF stimulation, ROS production was nearly undetectable. (F) In contrast, PpyNWs not subjected to EMF stimulation again showed significant ROS production in the tested cell population. (G) Corresponding graph describing the quantitation of ROS production in panels A–F. Values are shown as percentages normalized to the control. (H) Additional ROS data using H_2O_2 as a positive control to induce ROS. The graph confirms that both applied and stimulated DEX suppressed ROS production and that DEX retained its bioactivity after EMF stimulation. $^*P \leq 0.05$ and $^{**}P \leq 0.01$.

3000–5000 V/m range for the 15-turn coils. We emphasize that due to the high-frequency pulsed nature of the stimulation pattern these are the estimated peak EMF values during the 500 ns pulse duration. The time-averaged EMF values are much lower when considering the duty cycle and would be less than 5% of these values. The distance dependence of the electric field from the coil center followed that of the magnetic field. Note that for BV-2 cell culture experiments, the coil was placed on the bottom of the Petri dish since it was not possible to place the culture chamber within the coil. In such situations, the measured peak fields to which the Ppy substrates were exposed were between 3–20 G and 300–2500 V/m for the MF and EF, respectively.

3.3. Comparisons of DEX Release. Drug release characteristics of the PpyNWs to conventional flat Ppy films are shown in Figure 5.

Figure 5A reveals the results of drug release monitored over a 5 h period. Potentiostat stimulation of flat Ppy-AuNps was not significantly different from that of EMF stimulation. Upon exposure to EMF stimulation, there was a statistically significant increase in the release levels of PpyNWs compared to that of the flat Ppy film ($^*P \leq 0.05$). Also note that the EMF stimulation of PpyNWs-AuNps resulted in more release of DEX than did potentiostat stimulation.

The inclusion of gold nanoparticles greatly improved the loading capacity and the rate of release. This trend was preserved in both flat Ppy thin films and in the PpyNWs, when compared to the PSS-doped Ppy films. At 1, 7, and 16 days, these differences were almost double for both Ppy platforms ($^*P \leq 0.05$ between PpyNWs and $^{**}P \leq 0.01$ between flat Ppy). Also, PpyNWs showed a very significant enhancement of DEX release triggered by EMF stimulation when compared to flat Ppy (on days 1 and 16, $^{**}P \leq 0.01$, and on day 7, $^{***}P \leq 0.001$ between AuNPs; at days 7 and 16, $^{**}P \leq 0.01$ between PSSs studied, Figure 5B). Background release studies (no stimulation) showed that the outward diffusion of DEX was below 0.11 mg/cm^2 for PpyNWs and 0.3 mg/cm^2 for flat Ppy films on the last day of recording. This reveals a significant drug release of EMF stimulation compared to that without EMF stimulation. (on day 1, $^{**}P \leq 0.01$, and on days 7 and 16, $^{***}P \leq 0.001$ between PpyNWs; on day 1, $^*P \leq 0.05$, and on days 7 and 16, $^{**}P \leq 0.01$ between flat Ppy films, Figure 5C).

Figure S4 depicts the DEX release profiles of flat Ppy as a function of temperature. Some passive background release was

dx.doi.org/10.1021/la500033b | Langmuir 2014, 30, 7778–7788

found, but it did not reach the levels of active EMF stimulation. Further switching experiments where the EMF was turned on for 2 h and then turned off for 2 h are shown in Figure 5D. In such cases, DEX release fell off precipitously after the removal of EMF stimulation and was regained when EMF coupling was resumed. Such consistency over multiple unloading cycles demonstrated excellent reproducibility and reversibility that is a hallmark of controlled release.

3.4. XPS Confirmation of DEX Release. X-ray photoelectron spectroscopy (XPS) was used to verify the existence of DEX and to verify the escape of entrapped drug (Figure 6). XPS surface analysis was conducted on the PpyNWs before and after (16 days) pulsed electromagnetic stimulation. As expected, high-resolution spectra of F 1s and P 2p revealed changes in the peak magnitudes, denoting an obvious release of DEX upon exposure to the EMF. Specifically, these spectrographs detail signatures of fluorine and phosphorus elements in the DEX molecule, which essentially vanish after EMF stimulation. For PpyNWs-AuNps, the prestimulation F 1s and P 2p atomic percentages were 1.53 and 1.54%, respectively, while the poststimulations results were 0.00 and 0.17%. For PpyNWs-PSS, the prestimulation F 1s and P 2p atomic percentages were 0.60 and 1.31%, respectively, while the poststimulations results were 0.00 and 0.15%.

3.5. BV-2 Cell Responses to the Application of PpyNWs-AuNps. Two groups of toxin-challenged murine neonatal microglial cells (BV-2) were used to evaluate ROS production and to determine whether such damaged cells could be rescued via EMF-associated drug release. In one group, the challenge was bacterially derived LPS (Figure 7A–G), and in the other, the cells were directly insulted with hydrogen peroxide (Figure 7H).

BV-2 cells treated with LPS released pro-inflammatory cytokines and ROS via MAPK signaling pathways.[19] CM-H2DCFDA is one such indicator compound for ROS and was used as a metric for ROS production. LPS (1 μg/mL)-treated cells exhibited bright green fluorescence in the cytoplasm, marking the production of significant oxidative stress (Figure 7B). The addition of DEX (1 μg/mL) to these LPS-induced microglia effectively suppressed ROS production during the inflammatory cascade (Figure 7C). The DEX-doped PpyNWs-AuNps platform also suppressed inflammation by-products during EMF stimulation (Figure 7E). A weaker inhibition of ROS activity occurred when shorter stimulation times were applied (Figure 7D). In contrast, nonstimulated DEX/PpyNWs-AuNps films did not show signs of ROS scavenging (Figure 7F,G).

Similarly, exposure to 20 μg/mL H_2O_2 resulted in more ROS byproducts in BV-2 cells (Figure 7H). This enhanced production of ROS was reduced either by direct application of 10 μg/mL DEX or by 15 min of EMF stimulation to the DEX-coupled PpyNWs-AuNps. These findings were further corroborated by the results of iNOS measurements. Microglial cells were stained intensely with Cy3 (red fluorescent signal) when exposed to LPS in a dose-dependent manner (Figure 8). iNOS expression in BV-2 cells after LPS challenge (without stimulation) also showed positive Cy3 staining, which is in agreement with the ROS results (Figure 7). In contrast, EMF stimulation of DEX-conjugated PpyNWs-AuNps resulted in a strong suppression of iNOS, indicating a reduced level of nitric oxide.

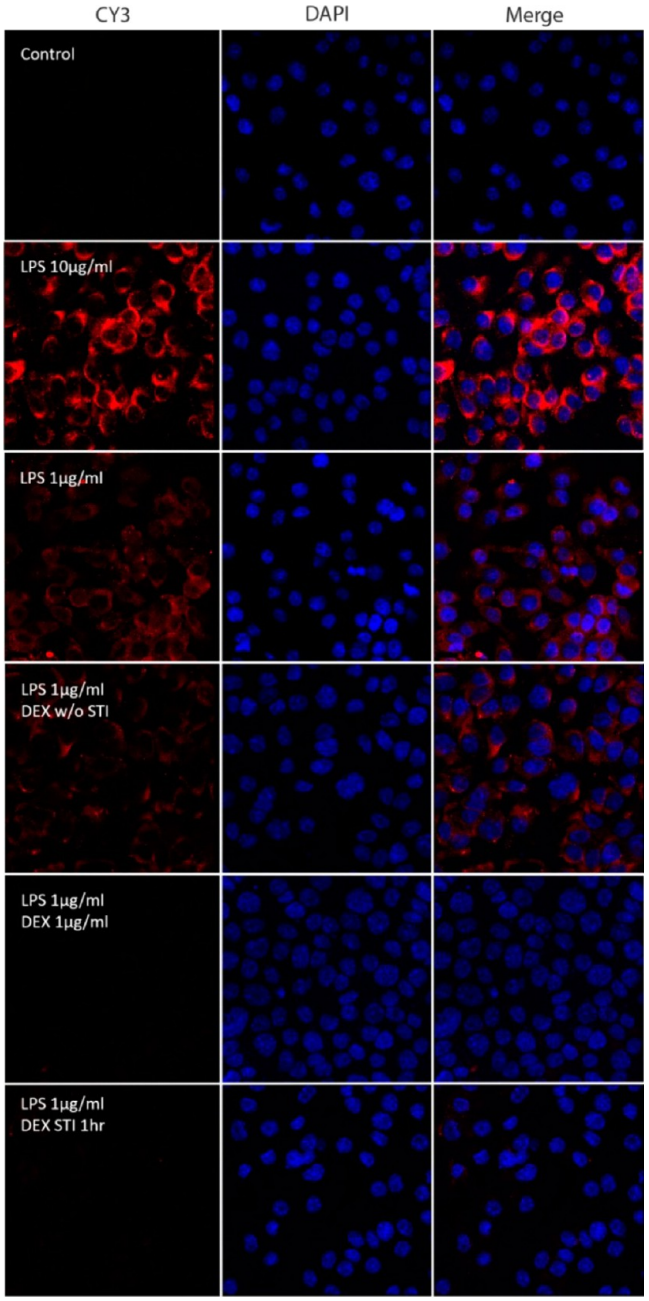

Figure 8. Confocal imaging of the iNOS expression after LPS induction in BV-2 cells. iNOS expression in BV-2 cells is shown with red fluorescence (CY3 column). Nuclear staining with DAPI is shown as a blue signal. The row labeled as control does not show any iNOS expression due to the absence of LPS treatment. In contrast, the row LPS 10μg/mL shows significant upregulation of iNOS, and the merged confocal micrograph details that the staining is primarily localized in the cytoplasm. Row LPS 1μg/mL shows less upregulation at a reduced LPS concentration while PpyNWs-AuNps not stimulated with EMF (DEX w/o STI) showed a similar response. However, when exposed directly to DEX (row LPS 1μg/mL/DEX 1μg/mL), results were comparable to the untreated control and highlighted the suppression of iNOS to LPS-challenged BV-2 cells. Finally, PpyNWs-AuNps stimulated with EMF (1 h) produced iNOS results comparable to direct DEX application.

4. DISCUSSION

Polypyrrole is an inherently conductive polymer that has shown promise as a "smart" biomaterial. The electroactive properties and biocompatibility of Ppy are desirable features in designing programmable drug-delivery systems. Previously, our group used topographically modified Ppy films that increased the available surface area for drug inclusion and release.[20] While the drug capacity was improved, these films were difficult to fabricate and highly porous, making them susceptible to damage. We have thus

dx.doi.org/10.1021/la500033b | Langmuir 2014, 30, 7778–7788

introduced another form of conductive Ppy by "shaping" the polymer into solid "nanowire" arrays for further functionalization.[21] Moreover, we propose the use of electromagnetic fields as the stimulus for Ppy drug release. This is a significant departure from all previous forms of drug-doped Ppy, in which direct electrical connection (i.e., wire electrodes) to the Ppy was required to induce current flow and subsequent drug release.

Experimental results showed that the PpyNWs-AuNps possessed excellent drug-carrying capabilities as well as a controllable switching response to electromagnetic fields. XPS analysis confirmed that the model drug, dexamethasone, was successfully incorporated onto the surface of the Ppy nanowires. When exposed to pulsatile EMFs, the DEX cargo was released from the Ppy surface, a process that was verified by changes in the surface chemistry and the free drug concentration. The amount of drug that could be eluted from EMF stimulation was superior to direct stimulation via a potentiostat.

While the mechanism of EMF-coupled drug release is still unclear, we hypothesize that the phenomenon is similar to Ppy stimulation via direct current. For instance, it is well known that Ppy undergoes an electrical and conformational change via an oxidation/reduction reaction in response to applied voltages. Furthermore, the electroactive Ppy swells during oxidation and shrinks (mechanical actuation) during reduction to satisfy charge balance.[22] This reversible volume change along with the electrostatics of moving charges within the Ppy governs how charged molecules move in and out of the Ppy (i.e., drug deposition and elution).[23] A multitude of cytokines/drugs such as nerve growth factors, analgesics, and adenosine triphosphate have been released in situ based on this functionality.[7−10] In the proposed polymer platform, charge balance is obtained when the anionic DEX is electrostatically entrapped within the cationic pyrrole chain during the electropolymerization process. When a sample is exposed to a time-varying EM field, an oscillating electric current is induced in the Ppy and is posited to drive the redox reaction. During the reduction state, charge neutralization of the pyrrole backbone eliminates the electrostatic bonding to the DEX, causing the DEX to migrate out of the Ppy matrix. Indeed, prior evidence has shown that DEX desorbs from Ppy in the reduction state.[24] Therefore, the cumulative reduction states that occur during the inductive cycling of Ppy facilitate DEX movement. The concomitant mechanical actuation or pumping action from the redox reaction may further play a role in forcing the DEX out of the Ppy. Not surprisingly, this polymer electroactive effect should be more pronounced if the conductivity of the Ppy is enhanced, which was indeed observed when the Ppy nanowires were impregnated with gold. As a result, it appears that DEX elution occurs regardless of whether current flow is direct or electromagnetically induced.

It has been noted that Ppy is susceptible to overoxidation whereby the electroactivity can diminish due to high applied voltages or continued stimulation.[25] This fatigue behavior was not detected as evidenced by the prolonged DEX release over a period of 16 days in vitro. The extended electrochemical stability of PpyNWs-AuNps may be partially due to the low duty cycle of the applied EM fields and its rapid oscillatory nature or by the enhanced conductivity conferred by the gold nanoparticles. For instance, the addition of multiwalled carbon nanotubes improves the conductivity and electrostability of Ppy neural prosthetic coatings.[26] However, induction may cause Joule heating and subsequent drug release, an observation that was described for carbon nanotubes.[14] To address passive thermal effects, we performed additional studies at elevated temperature (37 °C). Results show that temperature played only a small role in the release kinetics. Follow-up cyclical stimulation also revealed that DEX was released only during "on" stimulation states. It is further unlikely that pH changes were responsible for drug elution since these experiments were conducted in physiologically buffered solutions.

To verify the bioactivity of the released DEX cargo, we performed several cell culture assays using the BV-2 glial line exposed to lipopolysaccharide (LPS) toxin. Lipopolysaccharide-challenged microglia have been shown to induce neurotoxicity through the production of pro-inflammatory mediators such as tumor necrosis factor-α, interleukin-1β(IL-1β), ROS, and iNOS, which catalyze the production of nitric oxide (NO).[27] Dexamethasone is known to suppress the formation of ROS and iNOS.[19] Since a focus area within our laboratory is neurodegenerative diseases of the central nervous system (CNS) (reviewed in ref 20), we chose this in vitro neuroinflammatory model to assess the therapeutic activity of EMF-released DEX. The results showed that the addition of DEX (1 μg/mL) to LPS-exposed microglia suppressed ROS production. Similarly, the DEX-doped PpyNWs-AuNps platform also suppressed inflammation byproducts during EMF stimulation. A weaker inhibition of ROS activity occurred when shorter stimulation times were applied. In contrast, the nonstimulated DEX/PpyNWs-AuNps films did not confer signs of ROS scavenging. Similarly, exposure to the H_2O_2 positive control resulted in ROS byproducts in BV-2 cells. This production of ROS was also reduced either by direct application of 10 μg/mL DEX or with 15 min of EMF stimulation to the DEX-coupled PpyNWs-AuNps. These findings were consistent with iNOS measurements, with a marked reduction in iNOS expression in the presence of soluble DEX. While we cannot eliminate the possibility that EMF alone may reduce ROS-associated damage in BV-2 cells, this is highly unlikely since the nanosecond pulse widths and stimulation times used were much shorter than the EMF waveforms commonly employed in bioelectromagnetics.[28] Therefore, we conclude that the mitigation of the inflammatory cascade was due to the availability of free DEX.

Even as the proposed geometric scheme of Ppy improves with drug-loading capacity, the amount of drug delivered may still be considered to be miniscule in comparison to systemic delivery. However, the latter is not the aim of nanomedicine. Rather, the intent of nanoscaled reservoirs is to deliver extraordinarily high concentrations of potent drugs to a localized microenvironment in order to produce therapeutic responses in adjacent, contiguous cells. In essence, nanoconstruction aims to release drugs into only specified target areas while escaping systemic circulation and side effects, a critical advancement in therapies involving potent or toxic drug cargos. Examples of such indications include early detected tumors, a restricted lesion in the nervous system (such as a localized region of acute CNS embolism or trauma), and the local region of small-scale crush injury to CNS or PNS axons that completely inhibit action potential propagation across the injury zone. These minor spatial defects produce profound and catastrophic behavioral, functional, and cognitive consequences.[29−31] Here we show that the release of drugs from PpyNWs can occur for more than 2 weeks and may serve as an ideal candidate for such applications.

We finally note that the reported EMF stimulation protocol is not fully optimized, and we are refining methods in which this release system can be employed for broad biomedical and pharmaceutical applications. As the putative mode of drug

release is EMF-Ppy induction coupling, we aim to develop oscillating waveforms that maximize the induction current without significant Joule heating. This includes varying EMF pulsing schemes, frequencies, and coil geometries. The phenomenon of Joule heating requires special attention in vivo since the thermal energy must be dissipated. Additional design parameters will also account for the attenuation of the EM signal through skin and connective tissues. Various theoretical and empirical models that consider tissue permeability, conductivity, and imposed EMF frequency have been developed and will be used as a reference for design.[32] However, the pulsing frequencies used in the present system are effective in vitro within a couple of centimeters of the coil center and will serve as a basis for further in vivo study. Future improvements may also include synthesizing degradable forms of Ppy which may be resorbed within the body. Nonetheless, we reveal for the first time that a Ppy system can be used as a type of programmable drug-delivery reservoir that responds to electromagnetic fields. This action at a distance potentially provides a new direction for noninvasive controlled drug release.

5. CONCLUSIONS

Conductive polymer polypyrrole was fashioned into a nanowire architecture and doped with the drug dexamethasone. This geometry enabled high-capacity drug entrapment and subsequent sustained release for over 2 weeks. More importantly, the release of dexamethasone could be triggered on demand via an externally applied pulsed electromagnetic field. Dexamethsone remained bioactive, as demonstrated by its ability to ameliorate damage to toxin-challenged glial cells. This is the first demonstration of a noninvasive mode of drug delivery using polypyrrole. This form of programmable drug release has significant clinical implications.

■ ASSOCIATED CONTENT

Supporting Information

Fabrication of novel PpyNWs and their incorporation into and release from DEX. This material is available free of charge via the Internet at http://pubs.acs.org.

■ AUTHOR INFORMATION

Corresponding Author

*E-mail: cpr@purdue.edu. Phone: 765-494-7600. Fax: 765-494-7605.

*E-mail: yncho@ncc.re.kr. Phone: +82-31-920-2379. Fax: +82-31-920-2542.

Present Address

(Y.C.) New Experimental Therapeutics Branch, National Cancer Center 809 Madu-1dong, Ilsandong-gu, Goyang-si, Gyeonggi-do 410-769, Korea.

Author Contributions

The manuscript was written through the contributions of all authors. All authors have given approval to the final version of the manuscript.

Notes

The authors declare no competing financial interest.

■ ACKNOWLEDGMENTS

We appreciate the professional technical assistance of Michel Schweinsberg with the graphics and the assistance of Jennifer Danaher in manuscript preparation. We are grateful for the generous donation of BV-2 cells by Dr. Jau-Shyong (John) Hong and Mrs. Belinda C. Wilson (NIH, neuropharmacology group). These data are in partial fulfillment of the Doctoral Degree of W.G. This work was performed in its entirety within the Center for Paralysis Research, Purdue University College of Veterinary Medicine. All work was performed in compliance with all university, state, and federal guidelines on the use of hazardous chemicals. We also thankfully acknowledge the financial support from the General Funds of the Center for Paralysis Research, The State of Indiana, and a generous endowment from Mrs. Mari Hulman George.

■ REFERENCES

(1) Stuart, M. A.; Huck, W. T.; Genzer, J.; Muller, M.; Ober, C.; Stamm, M.; Sukhorukov, G. B.; Szleifer, I.; Tsukruk, V. V.; Urban, M.; Winnik, F.; Zauscher, S.; Luzinov, I.; Minko, S. Emerging applications of stimuli-responsive polymer materials. *Nat. Mater.* **2010**, *9*, 101−113.

(2) Kang, H.; Trondoli, A. C.; Zhu, G.; Chen, Y.; Chang, Y. J.; Liu, H.; Huang, Y. F.; Zhang, X.; Tan, W. Near-infrared light-responsive core-shell nanogels for targeted drug delivery. *ACS Nano* **2011**, *5*, 5094−5099.

(3) Schmaljohann, D. Thermo- and pH-responsive polymers in drug delivery. *Adv. Drug Delivery Rev.* **2006**, *58*, 1655−1670.

(4) George, P. M.; Lyckman, A. W.; Lavan, D. A.; Hegde, A.; Leung, Y.; Avasare, R.; Testa, C.; Alexander, P. M.; Langer, R.; Sur, M. Fabrication and biocompatibility of polypyrrole implants suitable for neural prosthetics. *Biomaterials* **2005**, *26*, 3511−3519.

(5) Cho, Y.; Borgens, R. B. Biotin-doped porous polypyrrole films for electrically controlled nanoparticle release. *Langmuir* **2011**, *27*, 6316−6322.

(6) Wang, X.; Gu, X.; Yuan, C.; Chen, S.; Zhang, P.; Zhang, T.; Yao, J.; Chen, F.; Chen, G. Evaluation of biocompatibility of polypyrrole in vitro and in vivo. *J. Biomed. Mater. Res.* **2004**, *68A*, 411−422.

(7) Richardson, R. T.; Thompson, B.; Moulton, S.; Newbold, C.; Lum, M. G.; Cameron, A.; Wallace, G.; Kapsa, R.; Clark, G.; O'Leary, S. The effect of polypyrrole with incorporated neurotrophin-3 on the promotion of neurite outgrowth from auditory neurons. *Biomaterials* **2007**, *28*, 513−523.

(8) Pyo, M.; Maeder, G.; Kennedy, R. T.; Reynolds, J. R. Controlled release of biological molecules from conducting polymer modified electrodes: The potential dependent release of adenosine 5′-triphosphate from poly (pyrrole adenosine 5′-triphosphate) films. *J. Electroanal. Chem.* **1994**, *368*, 329−332.

(9) Thompson, B. C.; Richardson, R. T.; Moulton, S. E.; Evans, A. J.; O'Leary, S.; Clark, G. M.; Wallace, G. G. Conducting polymers, dual neurotrophins and pulsed electrical stimulation—dramatic effects on neurite outgrowth. *J. Controlled Release* **2010**, *141*, 161−167.

(10) Leprince, L.; Dogimont, A.; Magnin, D.; Demoustier-Champagne, S. Dexamethasone electrically controlled release from polypyrrole-coated nanostructured electrodes. *J. Mater. Sci.: Mater. Med.* **2010**, *21*, 925−930.

(11) Murdan, S. Electro-responsive drug delivery from hydrogels. *J. Controlled Release* **2003**, *92*, 1−17.

(12) Hoare, T.; Santamaria, J.; Goya, G. F.; Irusta, S.; Lin, D.; Lau, S.; Padera, R.; Langer, R.; Kohane, D. S. A magnetically triggered composite membrane for on-demand drug delivery. *Nano Lett.* **2009**, *9*, 3651−3657.

(13) Gumhye, J.; Yun, Y. S.; Jinseok, B.; Kon, K. J. Electrically Actuatable Smart Nanoporous Membrane for Pulsatile Drug Release. *Nano Lett.* **2011**, *11*, 1284−1288.

(14) Wu, C.-H.; Cao, C.; Kim, J. H.; Hsu, C.-H.; Wanebo, H. J.; Bowen, W. D.; Xu, J.; Marshall, J. Trojan-Horse Nanotube On-Command Intracellular Drug Delivery. *Nano Lett.* **2012**, *12*, 5475−5480.

(15) Cho, Y.; Borgens, R. B. The preparation of polypyrrole surfaces in the presence of mesoporous silica nanoparticles and their biomedical applications. *Nanotechnology* **2010**, *21*, 205102.

(16) Clark, G. M. The multiple-channel cochlear implant: the interface between sound and the central nervous system for hearing, speech, and

language in deaf people—a personal perspective. *Philos. Trans. R. Soc., B* **2006**, *361*, 791−810.
(17) Luo, X.; Matranga, C.; Tan, S.; Alba, N.; Cui, X. T. Carbon nanotube nanoreservior for controlled release of anti-inflammatory dexamethasone. *Biomaterials* **2011**, *32*, 6316−6323.
(18) Webber, M. J.; Matson, J. B.; Tamboli, V. K.; Stupp, S. I. Controlled release of dexamethasone from peptide nanofiber gels to modulate inflammatory response. *Biomaterials* **2012**, *33*, 6823−6832.
(19) Huo, Y.; Rangarajan, P.; Ling, E.-A.; Dheen, S. T. Dexamethasone inhibits the Nox-dependent ROS production via suppression of MKP-1-dependent MAPK pathways in activated microglia. *BMC Neurosci.* **2011**, *12*, 49.
(20) Cho, Y.; Borgens, R. B. Polymer and nano-technology applications for repair and reconstruction of the central nervous system. *Exp. Neurol.* **2012**, *233*, 126−144.
(21) Longa, Y. Z.; Lia, M. M.; Gub, C.; Wan, M.; Duvail, J. L.; Liu, Z.; Fan, Z. Recent advances in synthesis, physical properties and applications of conducting polymer nanotubes and nanofibers. *Prog. Polym. Sci.* **2011**, *36*, 1415−1442.
(22) Otero, T. F.; Martinez, J. G. Biomimetic intracellular matrix (ICM) materials, properties and functions. Full integration of actuators and sensors. *J. Mater. Chem. B* **2013**, *1*, 26−38.
(23) Green, R. A.; Lovell Nh Fau - Wallace, G. G.; Wallace Gg Fau - Poole-Warren, L. A.; Poole-Warren, L. A. Conducting polymers for neural interfaces: challenges in developing an effective long-term implant. *Biomaterials* **2008**, *29*, 3393−3399.
(24) Wadhwa, R.; Carl, L.; Xinyan, C. Electrochemically controlled release of dexamethasone from conducting polymer polypyrrole coated electrode. *J. Controlled Release* **2006**, *110*, 531−541.
(25) Li, Y.; Wang, P.; Wang, L.; Lin, X. Overoxidized polypyrrole film directed single-walled carbon nanotubes immobilization on glassy carbon electrode and its sensing applications. *Biosens. Bioelectron.* **2007**, *22*, 3120−3125.
(26) Green, R. A.; Williams, C. M.; Lovell, N. H.; Poole-Warren, L. A. Novel neural interface for implant electrodes: improving electroactivity of polypyrrole through MWNT incorporation. *J. Mater. Sci.: Mater. Med.* **2008**, *19*, 1625−1629.
(27) Zhong, L. M.; Zong, Y.; Sun, L.; Guo, J. Z.; Zhang, W.; He, Y.; Song, R.; Wang, W. M.; Xiao, C. J.; Lu, D. Resveratrol inhibits inflammatory responses via the mammalian target of rapamycin signaling pathway in cultured LPS-stimulated microglial cells. *PloS One* **2012**, *7*, e32195.
(28) Shupak, N. M.; Prato, F. S.; Thomas, A. W. Therapeutic Uses of Pulsed magnetic-Field Exposure: A review. *Radio Sci. Bull.* **2003**, *307*, 9−32.
(29) Cho, K.; Wang, X.; Nie, S.; Chen, Z.; Shin, D. M. Therapeutic Nanoparticles for Drug Delivery in Cancer. *Clin. Cancer Res.* **2008**, *14*, 1310−1316.
(30) Arap, W.; Pasqualini, R.; Ruoslahti, E. Cancer treatment by targeted drug delivery to tumor vasculature in a mouse model. *Science* **1998**, *279*, 377−380.
(31) Allen, T. M.; Cullis, P. R. Drug delivery systems: entering the mainstream. *Science* **2004**, *303*, 1818−1822.
(32) Foster, K. Thermal and Nonthermal Mechanisms of Interaction of Radio-Frequency Energy with Biological Systems. *IEEE Trans. Plasma Sci.* **2000**, *28*, 15−23.